References

[1]Nashif, A. D., "New Method for Determining Damping Properties of Viscoelastic Materials," *Shock and Vibration Bulletin*, Vol. 36, April 1967, pp. 37-47.

[2]Jones, D. I. G., "An Alternative System for Measuring Complex Dynamic Moduli of Damping Materials," *Shock and Vibration Bulletin*, Vol. 45, 1975.

[3]Nashif, A. D., "Materials for Vibration Control in Engineering," *Shock and Vibration Bulletin*, Vol. 43, June 1973, pp. 145-151.

[4]Jones, D. I. G., "Temperature-Frequency Dependence of Dynamic Properties of Damping Materials," *Journal of Sound and Vibration*, Vol. 33, April 1974, pp. 451-470.

APRIL 1975 J. AIRCRAFT VOL. 12, NO. 4

Modeling Engine Static Structures with Conical Shell Finite Elements

Robert E. Kielb*

Wright-Patterson Air Force Base, Ohio

The conical shell element with nonsymmetric loading and displacement capabilities has excellent possibilities for application to engine static structures. The major benefit would be a dramatic reduction in computer time as compared with a plate model, however, a severe limitation is the inability to combine this element with any other element types. This paper shows a technique that can be used to bypass this element compatibility problem. The inherent difficulty lies in the degree-of-freedom peculiarities of the conical shell element. The nonsymmetric motion of this element is accomplished by expanding each degree of freedom in a Fourier series with respect to the azimuthal coordinate. The technique presented in this paper sums this Fourier series for each degree of freedom and connects it to the appropriate degree of freedom for the nonshell portions of the structure by using functional constraints. The methods used to make the elements compatible and the computer time, displacement, and stress comparisons with standard plate and beam models will be shown.

Nomenclature

f = line load density
G = functional constraint matrix
K = stiffness matrix
m = maximum harmonic number
n = harmonic number
P = forces
q = functional constraint forces
R = coefficients of functional constraints
U = displacements
z = axial
θ = rotational displacements
ϕ = azimuth position

Subscripts

c = connected
cu = crossed terms
n = harmonic number
r = radial
u = unconnected
z = axial
ϕ = azimuthal
O = zeroth harmonic

Superscripts

$*$ = anti-symmetric displacements
sd = standard displacement system
fc = Fourier coefficient system

Matrix Notation

$\{\ \}$ = column matrix
T = transpose
-1 = inverse

Received July 31, 1974; revision received December 20, 1974.

Index categories: Structural Static Analysis; Airbreathing Propulsion, Subsonic and Supersonic.

*Aerospace Engineer, Structures Group, Aeronautical Systems Division.

Introduction

THE main static structural components of gas turbine engines are assemblies of shells, plates, and beam substructures. The problem of analyzing these structures has always been a difficult one to solve. Until the 1960's, classical solutions had to be combined with testing and experience to predict the structural characteristics. With the advent of finite element solutions in the sixties, the ability to analyze engine static structures was greatly enhanced. The analyst was no longer limited to the few classical solutions available and had greater generality in geometry, loading conditions, material properties, and boundary conditions. Unfortunately, with this enhancement came the added expense of a finite element solution. Once the computer programs are available, the major expenses of a solution are computer time and input preparation time.

Presently, engine static structures are being analyzed by constructing finite element models consisting of plates and beams. An analysis of a model of this type is relatively expensive because of the large number of degrees of freedom required for accuracy. This increases both preparation and computer time. This paper proposes a new method of modeling engine static structures that decreases both computer time and preparation time when compared with a plate and beam analysis of similar accuracy. The method uses conical shell finite elements with nonsymmetric loading and deflection capability for the shell portions of the structure. Normal plate and beam elements are used for the nonshell portions. The degree-of-freedom problems encountered when these elements are combined are solved. The computer times for this method are compared with a standard plate and beam solution. The ability to take advantage of symmetry with these elements is also discussed.

The reason for the large computer times associated with plate and beam models of engine static structures is twofold. The shell portions of the structure require a large number of degrees of freedom for accuracy, and the combination of the shell and strut portions forces a large bandwidth for the resulting stiffness matrix. The shell portions of the structure require many elements that are essentially identical. Most programs are not able to take advantage of this element similarity. As a result, element stiffness generation time is another major procedure in which the possibility to decrease computer time exists.

Conical Shell Method

An axisymmetric finite element approach seems promising; however, most cannot be used because of the inability to handle nonsymmetric loads and deflections. A conical shell element[1] has been developed in which the loads and deflections are expanded in a Fourier series with respect to the azimuthal coordinate (see Fig. 1). Thus, the elements are axisymmetric in geometry but nonsymmetric in loads and deflections. This element seems to be very efficient because one of these elements can replace very many plate elements. Because of symmetry, displacement systems associated with the various harmonic orders are independent. Also, the displacement systems associated with the symmetric and antisymmetric loading conditions relative to the azimuthal origin are independent. These facts result in a large time savings over the plate models. In effect, many small displacement systems are being solved, rather than one large system.

In application of these elements to engine static structures, the problem arises of connecting the conical shell elements with other elements such as plates and beams. This has not been accomplished in the past because of the degree-of-freedom peculiarities of the conical shell element. The Fourier expansions for the six degrees of freedom of a grid circle are shown in Eqs. 1–6.

$$U_r = \sum_{n=0}^{m} U_{rn} \cos(n\phi) + \sum_{n=1}^{m} U_{rn}{}^* \sin(n\phi) \tag{1}$$

$$U_\phi = \sum_{n=1}^{m} U_{\phi n} \sin(n\phi) + U_{\phi o}{}^* - \sum_{n=1}^{m} U_{\phi n}{}^* \cos(n\phi) \tag{2}$$

$$U_z = \sum_{n=0}^{m} U_{zn} \cos(n\phi) + \sum_{n=1}^{m} U_{zn}{}^* \sin(n\phi) \tag{3}$$

$$\Theta_r = \sum_{n=1}^{m} \Theta_{rn} \sin(n\phi) + \Theta_{ro}{}^* - \sum_{n=1}^{m} \Theta_{rn}{}^* \cos(n\phi) \tag{4}$$

$$\Theta_\phi = \sum_{n=0}^{m} \Theta_{\phi n} \cos(n\phi) + \sum_{n=1}^{m} \Theta_{\phi n}{}^* \sin(n\phi) \tag{5}$$

$$\Theta_z = \sum_{n=1}^{m} \Theta_{zn} \sin(n\phi) + \Theta_{zo}{}^* - \sum_{n=1}^{m} \Theta_{zn}{}^* \cos(n\phi) \tag{6}$$

The unstarred parameter represents symmetric displacements and the starred parameters represent the antisymmetric displacements. The minus signs have been introduced with the equation for the convenience of having the stiffness matrixes for the starred and unstarred parameters identical. The unknowns in the solution vector are not the actual displacements but the harmonic coefficients of the Fourier expansion of displacement with respect to the aximuthal coordinate. Therefore, a degree of freedom of a nonshell element cannot find a corresponding degree of freedom on the shell element.

For a structure containing both conical shell elements and standard plate and beam elements, the normal stiffness-displacement-force equations can be partitioned into the form

$$\left[\begin{array}{c|c|c|c} K_c{}^{sd} & K_{cu}{}^{sd} & 0 & 0 \\ \hline K_{cu}{}^{sd\,T} & K_u{}^{sd} & 0 & 0 \\ \hline 0 & 0 & K_c{}^{fc} & K_{cu}{}^{fc} \\ \hline 0 & 0 & K_{cu}{}^{fc\,T} & K_u{}^{fc} \end{array}\right] \left\{\begin{array}{c} U_c{}^{sd} \\ \hline U_u{}^{sd} \\ \hline U_c{}^{fc} \\ \hline U_u{}^{fc} \end{array}\right\} = \left\{\begin{array}{c} P_c{}^{sd} \\ \hline P_u{}^{sd} \\ \hline P_c{}^{fc} \\ \hline P_u{}^{fc} \end{array}\right\} \tag{7}$$

Where the *sd* superscripts represent the standard displacement degrees of freedom and the *fc* superscripts represent the Fourier coefficient degrees of freedom. Equation (7) is not sufficient to solve the problem because of a lack of connectivity between the Fourier coefficient degrees of freedom and the standard displacement degrees of freedom. The *c* subscripts represent the components that must be connected and the *u* subscripts represent components that will remain unconnected. Before additional equations are added to the system to connect these degrees of freedom, standard condensation procedures[2] are used to reduce the system to only the components that must be connected. This results in

$$\left[\begin{array}{c|c} \bar{K}^{sd} & 0 \\ \hline 0 & \bar{K}^{fc} \end{array}\right] \left\{\begin{array}{c} U_c{}^{sd} \\ \hline U_c{}^{fc} \end{array}\right\} = \left\{\begin{array}{c} \bar{P}^{sd} \\ \hline \bar{P}^{fc} \end{array}\right\} \tag{8}$$

$$\bar{K}^{sd} = [K_c{}^{sd}] - [K_{cu}{}^{sd}][K_u{}^{sd}]^{-1}[K_{cu}{}^{sd\,T}] \tag{9}$$

$$\bar{K}^{fc} = [K_c{}^{fc}] - [K_{cu}{}^{fc}][K_u{}^{fc}]^{-1}[K_{cu}{}^{fc\,T}] \tag{10}$$

$$\bar{P}^{sd} = \{P_c{}^{sd}\} - [K_{cu}{}^{sd}][K_u{}^{sd}]^{-1}\{P_u{}^{sd}\} \tag{11}$$

$$\bar{P}^{fc} = \{P_c{}^{fc}\} - [K_{cu}{}^{fc}][K_u{}^{fc}]^{-1}\{P_u{}^{fc}\} \tag{12}$$

The connectivity can be achieved by writing equations of the form

$$\left[R^{sd} \vdots R^{fc}\right] \left\{\begin{array}{c} U_c{}^{sd} \\ \cdots \\ U_c{}^{fc} \end{array}\right\} = \{0\} \tag{13}$$

These equations can be thought of as functional constraints and are referred to as multipoint constraints in the NASTRAN theoretical manuals.

For example, consider the symmetric radial displacement of a conical shell ring. From Eq. (1) we know for a given azimuthal position ϕ, that

$$U_r{}^{sd} = U_{ro}{}^{fc} + \sum_{n=1}^{m} U_{rn}{}^{fc} \cos(n\phi) \tag{14}$$

If this equation is put in the form of Eq. (13), it can be seen that

$$[R^{sd}] = [-1] \tag{15}$$

and

$$[R^{fc}] = [1 \ \cos(\phi) \ \cos(2\phi) \ldots \cos(M\phi)] \tag{16}$$

Equation (13) can also be written in the form:

$$\{U_c{}^{sd}\} = [G]\{U_c{}^{fc}\} \tag{17}$$

where

$$[G] = -[R^{sd}]^{-1}[R^{fc}] \tag{18}$$

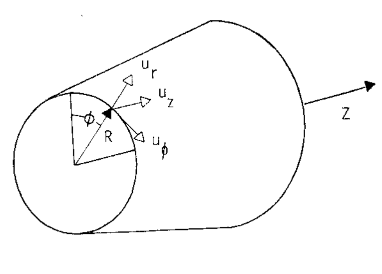

Fig. 1 Conical shell element coordinate system.

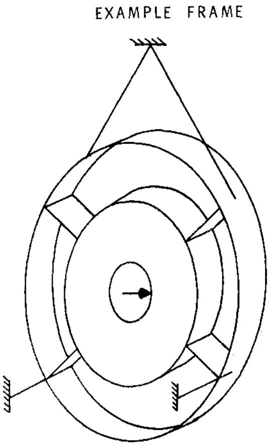

Fig. 2 Structure used for example problem.

Now Eq. (17) must be added to Eq. (8). The result is:

$$\begin{bmatrix} \bar{K}^{sd} & 0 & -I \\ 0 & \bar{K}^{fc} & G^T \\ -I & G & 0 \end{bmatrix} \begin{Bmatrix} U^{sd} \\ U^{fc} \\ q \end{Bmatrix} = \begin{Bmatrix} \bar{P}^{sd} \\ \bar{P}^{fc} \\ 0 \end{Bmatrix} \tag{19}$$

where q may be interpreted as the constraint forces on the U_c^{sd} degrees of freedom. Elimination of U_c^{sd} and q from the system results in:

$$[[\bar{K}^{fc}] + [G^T][\bar{K}^{sd}][G]]\{U^{fc}\} = \{\bar{P}^{fc}\} + [G^T]\{\bar{P}^{sd}\} \tag{20}$$

or

$$[K]\{U_c^{fc}\} = \{P\} \tag{21}$$

where

$$[K] = [\bar{K}^{fc}] + [G^T][\bar{K}^{sd}][G] \tag{22}$$

and

$$\{P\} = \{\bar{P}^{fc}\} + [G^T]\{\bar{P}^{sd}\} \tag{23}$$

By solving Eq. (21), U_c^{fc} is known and can be used in Eq. (17) to solve for U_c^{sd}. U_u^{sd} and U_u^{fc} can then be found by using Eq. (7).

It should be noted that Eq. (21) cannot be solved by separating the various harmonic orders. This is because the harmonic symmetry has been destroyed as a result of adding Eq. (17) to the system. However, once U_c^{fc} is known, harmonic symmetry can be used when solving Eq. (7) for U_u^{fc}. The entire solution procedure could be accomplished using both the starred and unstarred parameters in Eqs. (1-6). A better method is to perform symmetric and antisymmetric solutions and combine them to find the nonsymmetric solution. It might seem that the $[R^{sd}]$ matrix should be equal to $[I]$. This is not generally true because a single conical shell ring may be attached to

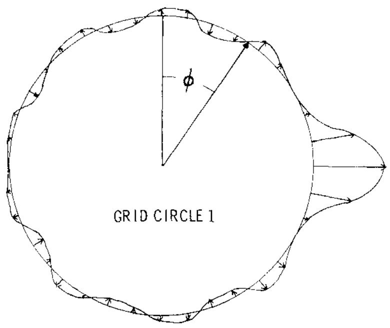

Fig. 4 Ten-term Fourier series representation of point load.

standard degrees of freedom at various azimuthal positions.

Example Problem

Rather than write a completely new program to test this method of analysis, it was decided to use NASTRAN as a test bed. NASTRAN was chosen because: 1) it has a nonsymmetric conical shell element in its library; 2) it can perform matrix partitioning; and 3) it will accept the additional constraining equations. NASTRAN will only allow a limited number of data card types when the conical shell element is used and will not allow the combination of this element with any other element. Substructuring can be used, however, to bypass the difficulty of getting data cards accepted and of combining the element with others. That is, all of the conical shell portions can be put in one substructure and all of the standard plate and beam portions can be put in the remaining substructure. The additional equation combining the structures can then be introduced into Phase II of the substructure analysis.

In choosing a demonstration problem for this analysis method, it was derived to have a simple structure yet include many features that would be encountered in the static structure of a gas turbine engine. Figure 2 shows the structure chosen. As can be seen, it includes two cylinders and one perforated circular plate connected by four struts and being supported by four beams. The analysis presented here includes a nonsymmetric loading condition duplicating a maneuver-type load where gyroscopic effects induce a side force through the bearing to the engine frame.

Figure 3 shows the structural idealization using conical shell elements in connection with plates and beams. The structure displays reflective symmetry about the plane of the azimuthal origin, therefore, only half the structure need be modeled. All of the elements included both bending and transverse shear stiffness. The thickness of the shells and plates is 0.1 in. and the beams are 1 in. × 1 in.

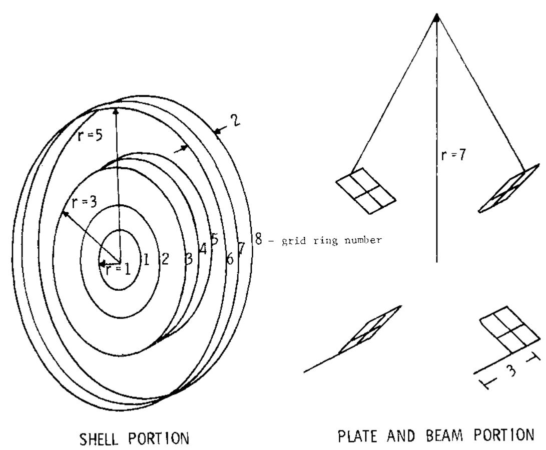

Fig. 3 Conical shell idealization.

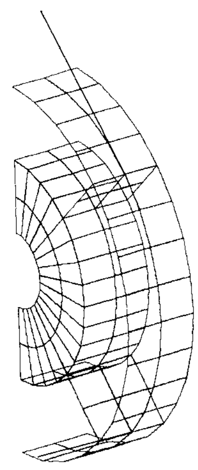

Fig. 5 Plate and beam idealization.

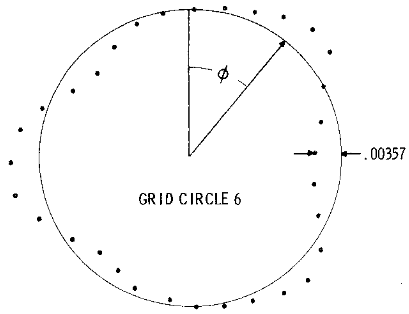

Fig. 6 Deformed shape of grid circle 6.

in cross section. The Fourier series representing the point load applied to the grid circle with 1 in. radius is listed below and shown in Fig. 4.

$$P_r(\phi) = \frac{2000}{\pi}(1 + \sin(\phi) - \cos(2\phi) - \sin(3\phi) + \cos(4\phi) + \sin(5\phi) - \cos(6\phi) - \sin(7\phi) + \cos(8\phi) + \sin(9\phi)) \quad (24)$$

It should be noted that the solution has been truncated at harmonic number nine. It was felt that this would keep the problem small, yet allow a complex displacement function. It was also desired to have accuracy similar to the standard plate. Figure 5 shows the idealization using standard plate and beam elements. The model consists of 104 plates and 2 beams. The element thicknesses and areas as well as the material properties were identical to the conical shell model. A point load was applied to the model as shown in Fig. 2. Both models were then run on NASTRAN (level 15) so that a comparison could be made between the two methods. The remainder of the paper discusses this comparison and makes conclusions as to the merit of each method.

In general, the results from the two methods were very similar. The deformed shape of both methods showed the same trends with small differences in magnitudes. Figure 6 shows the radial and tangential deformation of grid circle 6 for conical shell model. The plate and beam solution showed the same deformed shape, but had a maximum deflection at the 90° azimuthal position of 0.00306 as compared to 0.00357 for the conical shell. The comparison was similar for the remaining deflections. Figure 7 shows the

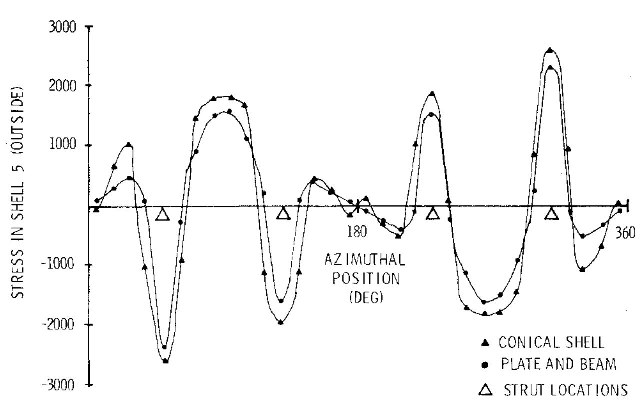

Fig. 7 Tangential stress comparison.

Table 1 Analysis parameters

Parameter	Conical shell method	Plate and beam method
Number of grid points	28	144
Number of elements	16	106
Degrees of freedom	588	864
Maximum stress in structure	10410	10660
Maximum deflection	0.01637	0.01367
Stiffness matrix generation time	19 sec	108 sec
Matrix decomposition time	52 sec	26 sec

comparison of tangential stress in shell 5 (located between grid circles 6 and 7; see Fig. 3). Again the two methods showed a similar relationship to the azimuthal position but with small differences in magnitude. The maximum in the conical shell model for this grid circle was 2646 and in the plate and beam model was 2338. The stresses in the remainder of the structure showed similar correlation. Table 1 gives a list of the significant parameters for the two analysis methods. From the number of elements and grid points, it can be seen that input preparation time would be less for the conical shell method. The impetus behind this paper was the large computer times associated with the plate and beam solutions. It was thought that the conical shell method could possibly decrease these times. As can be seen in Table 1, there was a dramatic reduction in stiffness matrix generation time. Even though the times for the conical shell method are based on having 10 harmonics, it should be noted that it would require 57 harmonics to equal the generation time of the plate and beam method. NASTRAN does not allow the user to reorder the harmonic coefficient degrees of freedom; therefore, the resulting *(K)* matrix [Eq. (22)] has a very large bandwidth. This is the reason for the large decomposition times of the conical shell method. If a program were written specifically for this method, this restriction could be eliminated and the decomposition times could be dramatically reduced.

Conclusion

It has been demonstrated that it is not only possible to connect the conical shell element with non-shell elements, but that results can be obtained comparable to those for a plate and beam model by using only 10 harmonics. It is possible to obtain a large time savings using the conical shell method as a result of a dramatic reduction in stiffness matrix generation time. However, it is not desirable to apply this method to NASTRAN because of the many limitations encountered. For this method to be economically wise, a program would have to be written that would automate the matrix algebra in Eqs. (7–23). It would also be desirable to have the program optimize the bandwidth of the K matrix in Eq. (22). This method would be applicable to structures that are comprised mainly of shells with a few non-shell portions. If only a small portion of the structure is comprised of shells, the standard plate and beam method would be advantageous.

References

[1]MacNeal, R. H., *Nastran Theoretical Manual,* SP-221(01), April 1972, pp. 5.9-1–5.9-35, NASA.

[2]Przemieniecki, J. S., *Theory of Matrix Structural Analysis,* McGraw-Hill, New York, 1968, pp. 147–148.

[3]Ref. 1, pp. 3.5-1—3.5-3.